Full Paper

Propellants, Explosives, Pyrotechnics

DOI: 10.1002/prep.201800261

Investigation into the Temperature Adaptability of HNIW-based PBXs

Guanchao Lan,[a] Shaohua Jin,[a] Baochao Jing,[a] Yu Chen,*[a] Dongxu Wang,*[b] Jinxin Li,[c] Na Wang,[c] and Minglei Chen[c]

Abstract: 2,4,6,8,10,12-Hexanitro-2,4,6,8,10,12-hexaazaisowurtzitane (HNIW) based polymer bonded explosives (PBXs) were prepared through an aqueous suspension method using cellulose acetate butyrate (CAB) or fluorine rubber F_{2311} as a binder. Then the variation rules of size, mass, surface micro-topography, mechanical properties, thermal decomposition performance and mechanical sensitivity of the samples were investigated experimentally before and after high temperature (HT), low temperature (LT), high temperature cycle (HTC) and temperature shock (TS) tests, respectively. The results showed that the PBX columns, with the change rates of size and mass less than 1 %, were still at an acceptable level after temperature adaptability tests, and that the surface unevenness of the PBX samples followed the descending order of HT > HTC > LT > TS, which was in a good agreement with the order of mass loss. Moreover, the stability of the samples might be decreased by temperature adaptability tests, among which TS had the largest effect on both HNIW/CAB and HNIW/F_{2311}. And a correlation between mechanical sensitivity and mechanical properties was found out through that the mechanical sensitivity of the PBXs stayed almost unchanged with a slight increase in the tensile strength of the columns after HTC whereas at least one sensitivity was increased markedly with the decline of the tensile strength after HT, LT or TS.

Keywords: temperature adaptability · polymer bonded explosives (PBXs) · HNIW · CAB · F_{2311}

1 Introduction

The temperature environment is complicated and volatile during the storage, carriage and usage process of polymer bonded explosives (PBXs). Both change in size due to temperature variation and aging and damage produced inside explosives may exert an influence on security performance, mechanical properties and energy characteristics of PBXs, and then negatively impact the overall functionality of warhead and the security in utilization of weapon system. Therefore, it is of significance to investigate the temperature adaptability of PBXs.

Recently, large numbers of researches have focused on the temperature adaptability of PBXs under constant temperature, cyclic temperature or shock temperature, of which the test conditions are mostly determined by storage situations and usage requirements. Wei et al. [1] studied the thermal damage of HMX-based PBX by ultrasonic characterization after the thermal cycle and thermal shock tests between −40 °C and 75 °C, and investigated the mechanical properties and failure modes of the PBX experimentally before and after environment tests. The results showed that thermal cycle and thermal shock could induce the thermal damages of PBX which made the compressive strength decrease slightly and had an insignificant effect on tensile strength. Yin et al. [2] investigated temperature damage of boundary-limit pressed HMX-based PBX through high-low temperature cycle and temperature shock test, and studied the environment adaptability of damaged explosives by shock, vibration and depreciation experiment. The results showed that both temperature cycle and temperature shock caused crack damages of explosives, of which the latter one created more crack damages, and that there was no occurrence of explosion or combustion in the environment adaptability experiment of the damaged explosive. Zheng et al. [3] prepared PBXs with the component of HMX/HTPB/TDI and studied the internal damage, temperature and strain of shell exterior, and the change in size, density and mechanical properties of the explosives by temperature shock test and temperature cycle test of −55 °C ~ 70 °C to research the temperature adaption of cast PBX. The results showed that there was no obvious thermal damage in the cast PBXs and that the original damage did not extend obviously as well after temperature shock test and temperature cycle test. Moreover, the density of the explosive in-

[a] *G. Lan, S. Jin, B. Jing, Y. Chen*
School of Materials Science and Engineering, Beijing Institute of Technology, 100081, Beijing, China
**e-mail: bityuchen@bit.edu.cn*
[b] *D. Wang*
School of Mechatronical Engineering, Beijing Institute of Technology, 100081, Beijing, China
**e-mail: dadadolindsay@126.com*
[c] *J. Li, N. Wang, M. Chen*
Gansu Yin Guang Chemical Industry Group Co. Ltd., 730900, Baiyin, China

 © 2019 Wiley-VCH Verlag GmbH & Co. KGaA, Weinheim

creased by 0.001 $g \cdot cm^{-3}$, and the tensile strength and compressive strength increased by 0.12 MPa and 0.55 MPa, respectively. Zhang et al. [4] studied the crack formation rule and mechanism of A-IX-II explosive with different dimensions and charge densities via high-low temperature cycle test with different temperature ranges. The results showed that A-IX-II grain with high density and large dimension cracked more easily under temperature cyclic load. Liu et al. [5] investigated the effect of the environmental temperature on the explosive structure via temperature shock tests conducted on RDX-based pressed and DNAN-based cast explosives. The results showed that RDX-based pressed explosives were likely to generate micro cracks under the temperature test process and that the cracks probably concentrated at the largest outer bottom while the DNAN-based cast explosives were more insensitive to the intense temperature variations.

2,4,6,8,10,12-Hexanitro-2,4,6,8,10,12-hexaazaisowurtzitane (HNIW) is a high-energy material with cage structure, which can be regarded as a powerful explosive of the next generation [6]. In view of its superior detonation performance, HNIW, popularly known as CL-20, has been widely used as the main explosive in many PBX formulations close to the practical application [7–10]. Nowadays, most studies around HNIW-based PBXs concentrate on the selection of additives, the improvement of coating process, and the exploration of coating mechanism. In contrast, the investigation into the temperature adaptability of HNIW-based PBXs has not been reported. In this study, the molding powders of HNIW-based PBXs were prepared through an aqueous suspension method using cellulose acetate butyrate (CAB, with a small amount of mixture of bis(2,2-dinitropropil)formal and bis(2,2-dinitropropil)acetal (BDNPF/A) added in as a plasticizer) or fluorine rubber F2311 as a binder. Then high temperature (HT), low temperature (LT), high temperature cycle (HTC) and temperature shock (TS) tests were conducted on the molding powders and the columns pressed from the powders at a certain pressure, respectively. On this basis, the variation rules of size, mass, surface micro-topography, mechanical properties, thermal decomposition performance and mechanical sensitivity of the samples were investigated experimentally before and after temperature environment tests for a comprehensive analysis of HNIW-based PBXs.

2 Experimental Details

2.1 Materials

HNIW (purity > 99.5 %, analyzed by high-performance liquid chromatography) was synthesized by our laboratory. CAB, F_{2311} and all the solvents used were analytical reagent grade.

2.2 Preparation of Binder Solutions

Two grams of CAB or F_{2311} was dissolved in 30 mL ethyl acetate at 50 °C for 12 h as the binder solution.

2.3 Preparation of HNIW-based PBX Molding Powders

HNIW-based PBX molding powders were prepared using an aqueous suspension method [11]. Firstly, fifty grams of HNIW was added into 100 mL water under agitation with a stirring rate of 600 rpm and then the suspension was slowly heated up to 50 °C in a water bath maintained for half an hour. Then the binder solution was added dropwise as the stirring rate was increased to 800 rpm. When the feeding process was done, the suspension was heated up to 65 °C and the stirring rate was decreased to 600 rpm. After the solvent was evaporated completely, the suspension was slowly cooled down to 50 °C and maintained for 15 min. After the solvent was evaporated completely, the suspension was continuously cooled down to ambient temperature. Then the stirring was stopped and PBX molding powders were separated using vacuum filtration and dried.

2.4 Processing of HNIW-based PBX Columns

The HNIW-based PBX molding powders were processed into columns with dimensions of Φ 20 mm × 20 mm using the method of compression molding with the pressure of 400 MPa and maintained at 25 °C for 1 h, under which the charge density of samples could reach 97 % of the theoretical maximum density.

2.5 Temperature Adaptability Tests

The test chamber for temperature adaptability tests had dimensions of 500 mm × 600 mm × 500 mm, of which the temperature was controlled by constant temperature oil bath. For each sample, 15 columns and 2.5 grams of molding powders were placed independently in the test chamber for a specific temperature adaptability test. After the temperature adaptability tests, the columns were used for the determination of size, mass and mechanical strength, and the powders were used for the analysis of surface micro-topography, thermal decomposition performance and mechanical sensitivity. Correspondingly, columns and molding powders with the same amount of each sample without temperature adaptability tests were used for the above performance characterization as the reference.

High temperature test was aimed at investigating the long storage performance of explosives at high temperature, using accelerated aging test to measure the life of PBXs under natural temperature conditions. It was a censoring life test, which could be used to calculate the storage

 © 2019 Wiley-VCH Verlag GmbH & Co. KGaA, Weinheim

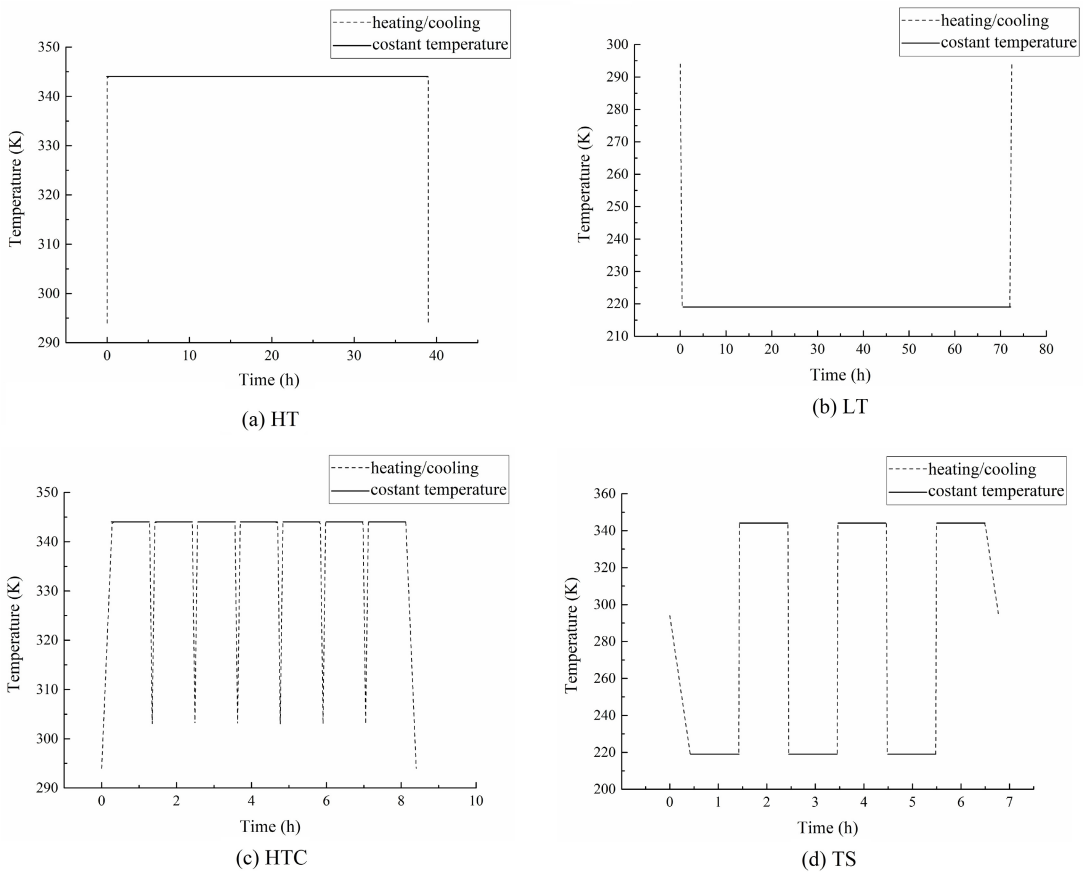

Figure 1. The setting curves of temperature variation for different temperature adaptability tests.

time at high temperature from that at ambient temperature through modified Arrhenius equation [12, 13]

$$t_0 = t_1 \cdot \gamma^{\frac{T_1 - T_0}{A}} \quad (1)$$

where t_0 and t_1 were the storage times at ambient temperature and high temperature, respectively; T_0 and T_1 were ambient temperature and high temperature of tests, valued as 294 K and 344 K in this study, respectively; γ was the temperature coefficient of reaction rate, valued as 2.7; A was the temperature variation corresponding to the reaction temperature, valued as 10 K. Accordingly, it was calculated that storage of 15 years at 294 K was equivalent to storage of 39 days at 344 K.

Low temperature test was conducted to inspect the influence of hardening, embrittlement or cracks caused by low temperature that was unfavorable for almost all the base materials. The PBX samples were placed into the test chamber at ambient temperature. Then the test temperature was decreased to 219 K and maintained for 72 hours. The temperature variation rate was controlled below 3 $K \cdot min^{-1}$ during the cooling process to avoid the effect of temperature shock.

High temperature cycle test was carried out to research the influence of the extreme temperature in the hottest area at the hottest month. The PBX samples were exposed at the temperature cycle of 303 ~ 344 K for seven times, and the highest temperature was maintained for 1 hour in each cycle, to simulate the times and the duration of each time of the extreme temperature when its occurrence probability was 1 %. The temperature variation rate was controlled below 10 $K \cdot min^{-1}$ during the heating and cooling process.

The extremes of low temperature in low temperature test and high temperature in high temperature cycle test, i. e., 219 K and 344 K, were used as the setting temperatures of temperature shock test to study the impact of alternating temperature on explosives. The temperature conversion was conducted three times, and the highest temperature and the lowest temperature were maintained for 1 h each time, respectively, with the conversion time no more than 1 min. The temperature variation rate was controlled below 10 $K \cdot min^{-1}$ at the initial and end stage of the test. The setting curves of temperature variation for different temperature adaptability tests are shown in Figure 1.

 © 2019 Wiley-VCH Verlag GmbH & Co. KGaA, Weinheim

3 Characterizations

The surface micro-topography, size, mass, mechanical properties, thermal decomposition performance and mechanical sensitivity of HNIW-based PBX samples were characterized before and after different temperature adaptability tests.

3.1 Measurement of Size and Mass

The size and mass of the columns were measured using screw micrometer and analytical balance, respectively. The final result was calculated through the averaging of the measured data.

3.2 Scanning Electrical Microscopy (SEM)

The surface micro-topography of the molding powders was observed using scanning electron microscope (MIRA3 XM, Tescan Co., Ltd., Brno, Czech Republic). The particle size of the sample observed was 0.85 ~ 1.18 mm.

3.3 Differential Scanning Calorimeter (DSC)

The thermal decomposition performance of the molding powders was characterized using differential scanning calorimeter (DSC 200 F3, Netzsch Group, Munich, Germany). The sample with the mass of 0.70 ± 0.01 mg was heated from 30 °C to 300 °C in dynamic nitrogen atmosphere of 40 mL·min^{-1} with a heating rate of 1, 2, 5 and 10 °C·min^{-1}, respectively. Each sample before or after a specific temperature adaptability test was analyzed three times with the mass of 0.70 ± 0.01 mg each time, and the median of the collected data was set as the final result.

Kissinger [14] and Ozawa [15] methods, described in the equation (2) and (3), respectively, were employed for the calculation of the kinetic parameters. Kissinger method,

$$\ln\left(\frac{\beta}{T_p^2}\right) = \ln\left(\frac{AR}{E_a}\right) - \frac{E_a}{RT_p} \tag{2}$$

Ozawa method,

$$\lg\beta = \lg\left[\frac{AE_a}{G(\alpha)R}\right] - 2.315 - 0.4567\frac{E_a}{RT_p} \tag{3}$$

where β was the heating rate, T_p was the peak temperature, E_a was the apparent activation energy, A was the pre-exponential factor, R was the gas constant valued as 8.314 J·K^{-1}·mol^{-1}, α was the conversion value that was the mass ratio of the reacted substance to the raw, and $G(\alpha)$ was the integral mechanism function. The pre-exponential factor (A) could be computed from the following equation,

$$A = \frac{\beta E_a}{RT_p^2}\exp\left(\frac{E_a}{RT_p}\right) \tag{4}$$

3.4 Determination of Mechanical Strength

The tensile strength of the columns was analyzed using Brazilian test [16–19] with an electromechanical universal testing machine (CMT4502, MTS Systems (China) Co., Ltd., Shanghai, China). A quasi-static radial compression load was imposed on the column with the loading rate of 0.5 mm·min^{-1} to generate an axial tensile stress in the central area enough to damage the column. Then the tensile strength, σ_t, could be calculated by the following equation [20],

$$\sigma_t = \frac{2P}{\pi dh} \tag{5}$$

where P was the acting force, d was the diameter of column and h was the thickness of the column. The final result was calculated through the averaging of the measured data.

The compression strength of the columns was analyzed with an electromechanical universal testing machine (CMT4502, MTS Systems (China) Co., Ltd., Shanghai, China). A quasi-static axial compression load was imposed on the column with the loading rate of 0.5 mm·min^{-1} until it was damaged. Then the compression strength, σ_c, could be calculated by the following equation,

$$\sigma_c = \frac{4P}{\pi d^2} \tag{6}$$

where P was the acting force and d was the diameter of column. The final result was calculated through the averaging of the measured data.

3.5 Determination of Mechanical Sensitivity

The impact sensitivity of the molding powders was tested with a 10 kg hammer dropping from the height of 250 ± 1 mm and the sample mass of 50 ± 1 mg at the temperature of 10 ~ 35 °C, keeping the humidity below 80 %. Each sample before or after a specific temperature adaptability test was determined 25 times with the mass of 50 ± 1 mg each time, and the explosion probability, P, was calculated by the following equation,

$$P = \frac{X}{25} \tag{7}$$

where X was the number of explosion during the tests.

The friction sensitivity of the molding powders was tested with the pressure of 3.92 MPa, the oscillation angle of

 © 2019 Wiley-VCH Verlag GmbH & Co. KGaA, Weinheim

Table 1. The variations of size and mass of the HNIW-based PBX columns before and after different temperature adaptability tests.

Test	HNIW/CAB ($\Delta d/d$)/%	($\Delta h/h$)/%	($\Delta V/V$)/%	($\Delta m/m$)/%
HT	−0.167 (±0.009)	−0.463 (±0.022)	−0.627 (±0.040)	−0.949 (±0.031)
LT	−0.092 (±0.008)	−0.175 (±0.008)	−0.320 (±0.024)	−0.138 (±0.005)
HTC	0.014 (±0.001)	−0.161 (±0.007)	−0.137 (±0.009)	−0.298 (±0.014)
TS	−0.016 (±0.001)	−0.071 (±0.003)	−0.105 (±0.005)	−0.009 (±0.001)
Test	HNIW/F_{2311} ($\Delta d/d$)/%	($\Delta h/h$)/%	($\Delta V/V$)/%	($\Delta m/m$)/%
HT	0.940 (±0.015)	−0.476 (±0.010)	0.972 (±0.040)	−0.618 (±0.023)
LT	−0.068 (±0.004)	−0.191 (±0.008)	−0.297 (±0.016)	−0.035 (±0.002)
HTC	0.162 (±0.006)	0.188 (±0.009)	0.604 (±0.021)	−0.225 (±0.012)
TS	−0.007 (±0.001)	−0.184 (±0.008)	−0.195 (±0.010)	−0.006 (±0.000)

$90 \pm 10^{\circ}$ and the sample mass of 30 ± 1 mg at the temperature of 10 ~ 35 °C, keeping the humidity below 80 %. Each sample before or after a specific temperature adaptability test was determined 25 times with the mass of 30 ± 1 mg each time, and the explosion probability, *P*, was calculated by the equation (7).

4 Results and Discussion

4.1 Size and Mass

The irreversible change in size of columns might cause skew or fracture of the charge and the variation in mass of columns would lead to cavities, cracks or defects, which had a significant impact on arms and ammunition. Therefore, the size and mass of the HNIW-based PBX columns were measured before and after different temperature adaptability tests, based on which the change rates of diameter, height, volume and mass of PBXs were calculated, as listed in Table 1. It was clear that all the absolute values of the change rates were within 1 %, which meant that the PBX columns were still at an acceptable quality level in size and mass after temperature adaptability tests according to American military standard MIL-STD-1751 [21].

The mass of columns was decreased after tests and the decline for HNIW/CAB was more than that for HNIW/F_{2311} in each case, from which it was deduced that the mass loss was probably due to the gasification and sublimation of small molecules such as BDNPF/A and PW in the formulations. For each formulation, the change rate of mass of columns after tests followed the descending order of HT > HTC > LT > TS, which was related to the processing time of temperature adaptability test.

Obviously, the variation rule for the change rate of size was more complicated compared with that for mass. Almost all the diameters, heights and volumes were decreased for HNIW/CAB while some of the parameters were increased for HNIW/F_{2311}. In the actual test process, change in size might be caused by the mass loss partially, in addition to which the variation in motion ability of molecules affected by the temperature variation was another probable reason. In this way, it could be explained that there was an expansion in diameter, height and volume of the HNIW/F_{2311} columns after HT or HTC in contrast to a contraction after LT or TS.

4.2 Surface Micro-topography

The surface micro-topography of the HNIW/CAB and HNIW/F_{2311} PBX samples before and after different temperature adaptability tests were displayed in Figure 2 and Figure 3, respectively. As shown in Figure 2 and Figure 3, change more or less had taken place in the surface micro-topography of the PBX samples after each temperature adaptability test. The untreated samples had a neat and smooth surface where the space between explosive crystals were filled with binders. By contrast, the surface of the samples became uneven, dotted with small holes and cavities, which was probably due to the gasification and sublimation of the additives on the surface. Furthermore, it was observed that the surface unevenness of the PBX samples followed the descending order of HT > HTC > LT > TS, which was consistent with the variation rule of mass loss. Considering that the mass loss was within 1 %, it would not cause serious damage to the surface of the samples.

4.3 Mechanical Properties

To investigate the variation of the mechanical properties of PBXs in different temperature environments, the tensile strength (σ_t) and compression strength (σ_c) of the HNIW-based PBX columns were determined before and after different temperature adaptability tests, as listed in Table 2. The results showed that the tensile of HNIW/CAB was generally superior to that of HNIW/F_{2311}. Besides, owing to the restriction of the upper limit of the testing machine, an ac-

 © 2019 Wiley-VCH Verlag GmbH & Co. KGaA, Weinheim

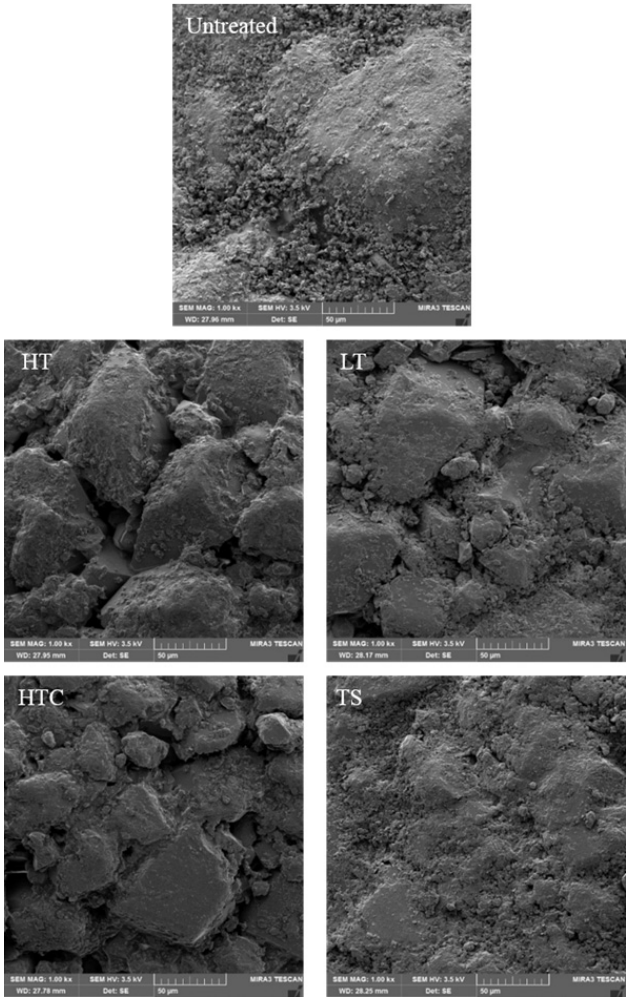

Figure 2. The surface micro-topography of the HNIW/CAB PBX samples before and after different temperature adaptability tests.

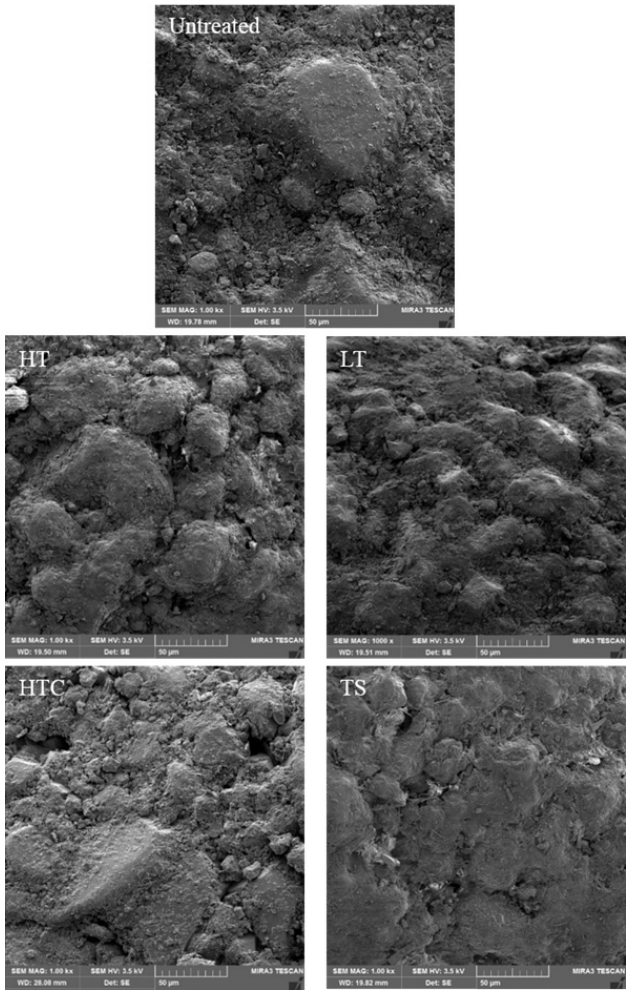

Figure 3. The surface micro-topography of the HNIW/F_{2311} PBX samples before and after different temperature adaptability tests.

curate comparison of the compression strength between the two formulations could not be achieved.

From Table 2, it was seen that the tensile strength of the PBX columns was decreased after HT, LT or TS. Contrarily, there was a slight increase in the tensile strength of the columns after HTC. It was deduced that discontinuous high-temperature processing might be propitious to the release of interior stress and defects. Furthermore, the tensile strength of the columns after LT was decreased by about 50% that exceeded the decreasing amplitude in other cases, indicating a bad low-temperature resistance of CAB as a binder. It was demonstrated by the variation of com-

Table 2. The tensile and compression strength of the HNIW-based PBX columns before and after different temperature adaptability tests.

Test	HNIW/CAB		HNIW/F_{2311}	
	σ_t/MPa	σ_c/MPa	σ_t/MPa	σ_c/MPa
Untreated	2.39 ($\pm$0.10)	10.71 ($\pm$0.53)	2.05 ($\pm$0.11)	$>$14.32
HT	2.33 ($\pm$0.10)	$>$14.32[a]	1.67 ($\pm$0.07)	$>$14.32
LT	1.19 ($\pm$0.04)	9.51 ($\pm$0.61)	1.99 ($\pm$0.10)	11.93 ($\pm$0.46)
HTC	2.40 ($\pm$0.11)	$>$14.32	2.10 ($\pm$0.12)	$>$14.32
TS	2.34 ($\pm$0.09)	$>$14.32	1.60 ($\pm$0.09)	$>$14.32

[a] The upper limit of the electromechanical universal testing machine was 4,500 N, and the corresponding compression strength was 14.32 MPa.

 © 2019 Wiley-VCH Verlag GmbH & Co. KGaA, Weinheim

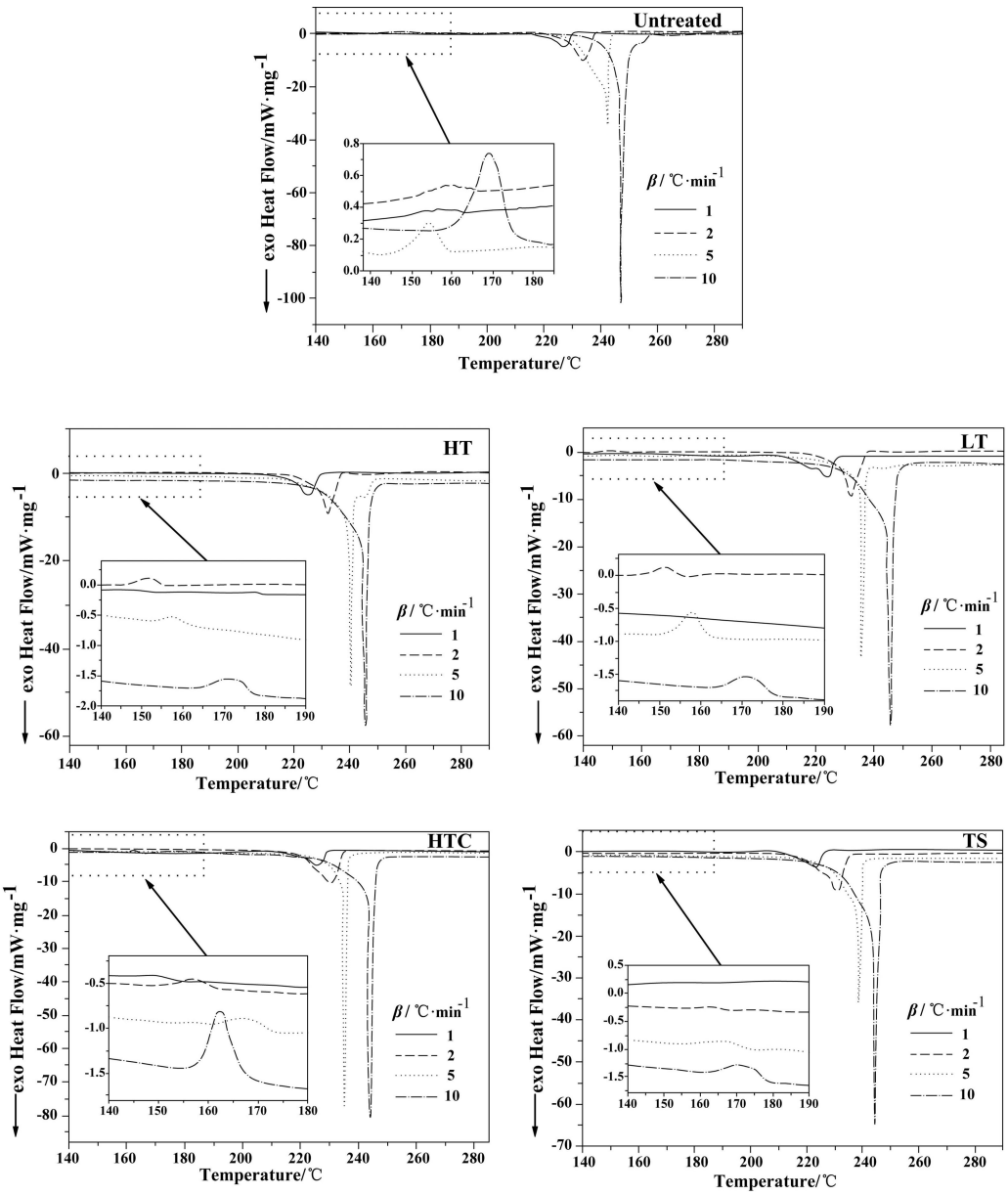

Figure 4. The DSC curves of the HNIW/CAB PBX samples before and after different temperature adaptability tests.

pression strength as well. Similarly, the decline of 20% in the tensile strength of the columns after HT or TS revealed that continuous high temperature might weaken the bonding capability of F_{2311}.

4.4 Thermal Decomposition Performance

The DSC curves of the HNIW/CAB and HNIW/F_{2311} PBX samples before and after different temperature adaptability tests were displayed in Figure 4 and Figure 5, respectively. It was found that there was no obvious difference in the shape of thermal decomposition peaks between the PBX samples before and after temperature adaptability tests. Generally, there were two characteristic peaks in the thermal decomposition process of the PBXs, an endothermal peak in the temperature range of 150~170 °C caused by the crystal polymorphic transformation of HNIW from ε to γ and an exothermal peak in the temperature range of 220~250 °C caused by the thermal decomposition of HNIW [22, 23].

The onset and peak temperatures (T_o & T_p) along with the heat flow (ΔH) of the DSC curves were listed in Table 3. It was seen that most of T_o decreased for most PBX samples after temperature adaptability tests compared with that for the untreated samples at a certain heating rate, which re-

 © 2019 Wiley-VCH Verlag GmbH & Co. KGaA, Weinheim

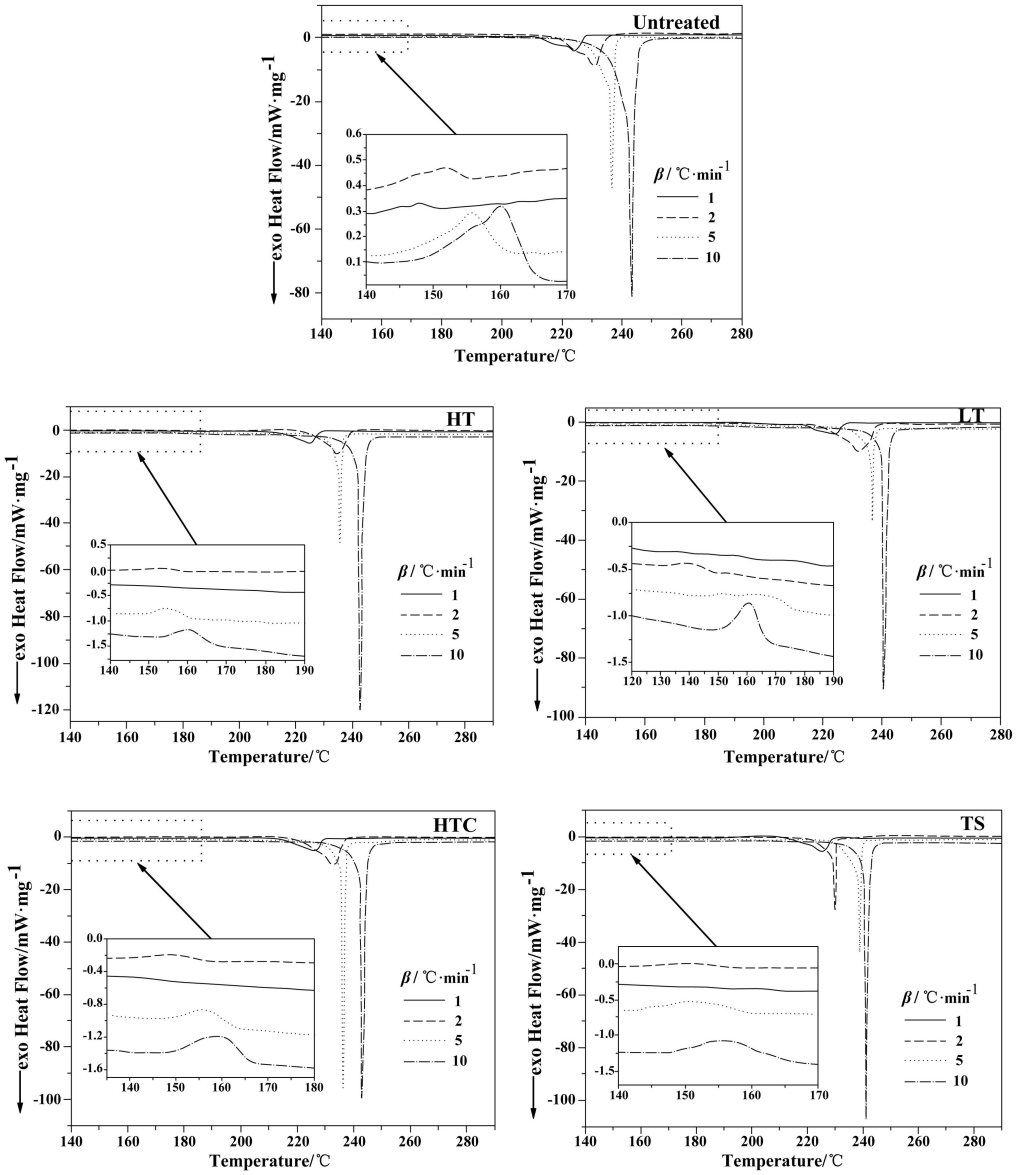

Figure 5. The DSC curves of the HNIW/ F_{2311} PBX samples before and after different temperature adaptability tests.

vealed that the heat insulation effect of the binder and the desensitizer on HNIW might become weak, resulting in a potential decline of the thermal stability of the whole system. Moreover, less heat was released during the thermal decomposition, probably because that decomposition reactions of some extent might have happened in the process of temperature adaptability tests to release some heat. Compared with the other tests, LT had a more remarkable effect on the decline of $|\Delta H|$, which meant that low temperature might destroy the homogeneity and consistency of the PBXs, causing the deficiency of the thermal decomposition reaction.

A linear fit of $\ln(\beta/T2\ p)$ with $1/T_p$ using the Kissinger method was made to calculate the E_a and A of the HNIW-based samples before and after different temperature adaptability tests. Similarly, another linear fit of $\ln\beta$ with $1/T_p$ using the Ozawa method was made to calculate the above parameters as well. The results were listed in Table 4, of which the correlation coefficients were all beyond 0.99, indicating the goodness of fit. It was obvious that the E_a calculated using the two methods were in close agreement with each other.

Generally, E_a reflected the reactive activity of thermal composition to assess the stability of the system. Specifically, the greater the value of E_a was, the less stable the

 © 2019 Wiley-VCH Verlag GmbH & Co. KGaA, Weinheim

Table 3. The onset temperature, the peak temperature and the heat flow of the DSC curves.

Test	β/°C·min^{-1}	HNIW/CAB			HNIW/F_{2311}		
		T_o/°C	T_p/°C	ΔH/J·g^{-1}	T_o/°C	T_p/°C	ΔH/J·g^{-1}
Untreated	1	221.54	223.07	−2651	215.07	224.17	−2557
	2	228.78	230.52	−2564	227.03	230.90	−2532
	5	237.09	238.50	−2252	236.55	236.69	−1206
	10	243.01	243.95	−1448	243.18	243.09	−1095
HT	1	219.84	227.10	−2644	214.08	224.85	−2549
	2	224.71	234.09	−2471	225.10	232.30	−2543
	5	238.60	242.17	−1906	235.36	235.36	−1107
	10	243.21	247.22	−1131	242.82	242.82	−1085
LT	1	216.75	225.49	−2320	214.26	223.73	−2532
	2	224.11	229.16	−2104	224.83	231.93	−2474
	5	235.87	240.05	−863	235.33	236.56	−762
	10	242.04	242.36	−1276	241.37	240.56	−740
HTC	1	220.45	224.04	−2631	214.93	224.28	−2521
	2	229.79	232.26	−2473	225.46	230.83	−2815
	5	237.07	236.04	−1163	235.52	236.73	−1001
	10	245.59	245.31	−1191	242.85	242.96	−958
TS	1	211.62	225.61	−2307	212.82	225.68	−2460
	2	224.51	230.57	−2397	224.04	232.66	−2409
	5	235.38	235.16	−1651	234.63	236.21	−1612
	10	242.72	243.74	−1346	240.75	243.06	−1505

Table 4. The kinetic parameters for the thermal decomposition of the HNIW-based PBX samples before and after different temperature adaptability tests.

Test	HNIW/CAB			HNIW/F_{2311}		
	E_a/kJ·mol^{-1}		A/s^{-1}	E_a/kJ·mol^{-1}		A/s^{-1}
	Kissinger	Ozawa		Kissinger	Ozawa	
Untreated	226.88	223.75	1.33×10^{21}	257.83	253.26	2.41×10^{24}
HT	237.68	234.09	1.19×10^{22}	275.58	270.08	1.74×10^{26}
LT	249.89	245.65	3.36×10^{23}	271.77	265.93	4.16×10^{25}
HTC	228.42	225.24	1.87×10^{21}	260.76	255.97	4.89×10^{24}
TS	268.70	263.55	3.30×10^{25}	285.89	279.88	1.90×10^{27}

whole system would be. It was found that all the heat-treated PBX samples had a higher E_a compared with the untreated one, which indicated a probable decline of the stability of PBXs after temperature adaptability tests. Among the tests, TS exerted the largest impact on both HNIW/CAB and HNIW/F_{2311}. On the contrary, the influence of HTC was negligible with a slight rise in E_a.

Table 5. The mechanical sensitivity of the HNIW-based PBX samples before and after different temperature adaptability tests.

Test	HNIW/CAB		HNIW/F_{2311}	
	P_{IS}/%	P_{FS}/%	P_{IS}/%	P_{FS}/%
Untreated	60	44	60	32
HT	88	52	92	56
LT	88	48	68	36
HTC	64	44	64	32
TS	88	48	88	44

4.5 Mechanical Sensitivity

The impact sensitivity (IS) and the friction sensitivity (FS) of the HNIW-based PBX samples before and after different temperature adaptability tests, characterized by the explosion percentage P, were listed in Table 5. The results showed that there was a remarkable increase in at least one of the two sensitivities for the PBX samples using CAB or F_{2311} as a binder after HT, LT or TS whereas the mechanical sensitivity for those after HTC stayed almost unchanged. It was similar to the variation rule of mechanical strength, probably because the decline of mechanical properties of binders caused by aging and the rise in interior stress and defects in the process of temperature adaptability tests increased the number and the spread probability of hot spot, which made the PBXs more sensitive to mechanical stimulus.

 © 2019 Wiley-VCH Verlag GmbH & Co. KGaA, Weinheim

5 Conclusions

(1) For the HNIW-based PBXs, both the change rates of size and mass had an absolute value within 1 %, suggesting that the columns were still at an acceptable level after temperature adaptability tests.

(2) The surface of the HNIW-based PBXs became uneven with some small holes and cavities, which might be caused by the mass loss after temperature adaptability tests. The surface unevenness of the PBX samples followed the descending order of HT > HTC > LT > TS, consistent with the order of mass loss as well.

(3) The tensile strength of the HNIW-based PBX columns was decreased after HT, LT or TS while there was a slight rise in the tensile strength of the columns after HTC, suggesting that discontinuous high-temperature processing might be propitious to the improvement of mechanical properties. As a binder, CAB had a bad low-temperature resistance, whereas continuous high temperature was unbearable to F_{2311}.

(4) The thermal analysis suggested that there might be a decline in the stability of the HNIW-based PBXs after temperature adaptability tests. Compared to the other tests, TS exerted a larger impact on both HNIW/CAB and HNIW/F_{2311}.

(5) The mechanical sensitivity of the HNIW-based PBXs remained almost unchanged after HTC while at least one sensitivity was increased remarkably after HT, LT or TS. The similarity in the variation rule between mechanical strength and mechanical sensitivity indicated that the former had a probable influence on the latter.

Acknowledgement

We acknowledge the Fundamental Research Funds for the Central Universities.

References

[1] X. W. Wei, X. Y. Zhou, X. Z. Tu, P. Wang, Thermal environment adaptability of HMX based PBX, *Chin. J. Explos. Propellants* **2012**, *35*, 15–17.
[2] J. T. Yin, B. H. Yuan, P. J. Niu, Y. Liu, J. Chen, Experimental study on the explosive damage and environment adaptability of damaged explosive, *Chin. J. Explos. Propellants* **2008**, *31*, 78–80.
[3] B. H. Zheng, M. Yin, C. Z. Geng, X. Z. Chen, T. Liu, D. Y. Gao, Y. Tang, G. Luo, Temperature adaptability of cast PBX under restriction of shell, *Chin. J. Energet. Mater.* **2017**, *25*, 232–239.
[4] D. M. Zhang, F. Han, L. Jia, L. J. Zhang, H. Chang, Q. Pan, K. Y. Wang, Q. Wang, J. Tu, Study on crack formation mechanism of pressed charge A-IX-II under temperature cyclic load, *Chin. J. Explos. Propellants* **2016**, *39*, 89–93.
[5] R. P. Liu, H. X. Wang, H. Wang, Q. L. Jiang, J. Gao, Y. M. Luo, K. Zhao, Effect of environment temperature on different explosive structures, *Sci. Technol. Eng.* **2014**, *14*, 274–277.
[6] U. R. Nair, R. Sivabalan, G. M. Gore, M. Geetha, S. N. Asthana, H. Singh, Hexanitrohexaazaisowurtzitane (CL-20) and CL-20-based formulations, *Combust. Explos. Shock Waves* **2005**, *41*, 121–132.
[7] D. M. Hoffman, Fatigue of LX-14 and LX-19 plastic bonded explosives, *J. Energ. Mater.* **2000**, *18*, 1–27.
[8] J. Li, T. B. Brill, Nanostructured energetic composites of CL-20 and binders synthesized by sol gel methods, *Propellants Explos. Pyrotech.* **2006**, *31*, 61–69.
[9] S. Thiboutot, P. Brousseau, G. Ampleman, D. Pantea, S. Côté, Potential use of CL-20 in TNT/ETPE-based melt cast formulations, *Propellants Explos. Pyrotech.* **2008**, *33*, 103–108.
[10] S. S. Samudre, U. R. Nair, G. M. Gore, P. K. Sinha, A. K. Sikder, S. N. Asthana, Studies on an improved plastic bonded explosive (PBX) for shaped charges, *Propellants Explos. Pyrotech.* **2009**, *34*, 145–150.
[11] D. X. Wang, S. S. Chen, S. H. Jin, Q. H. Shu, Z. M. Jiang, F. Q. Shang, J. X. Li, Investigation into the coating and desensitization effect on HNIW of paraffin wax/stearic acid composite system, *J. Energ. Mater.* **2016**, *34*, 26–37.
[12] M. Roth, M. R. Younginer, Prediction of the effects of storage on ARP propellant by means of chemical analysis, New Jersey, Picatinny Arsenal, **1962**.
[13] L. L. Rouch Jr., J. N. Maycock, Explosive and pyrotechnic aging demonstration, Washington, D.C., NASA, **1976**.
[14] H. E. Kissinger, Reaction kinetics in different thermal analysis, *Anal. Chem.* **1957**, *29*, 1702–1706.
[15] T. Ozawa, A new method of analyzing thermogravimetric data, *Bull. Chem. Soc. Jpn.* **1965**, *38*, 1881–1886.
[16] S. J. P. Palmer, J. E. Field, The deformation and fracture of β-HMX, *Proc. R. Soc. London A* **1982**, *383*, 399–407.
[17] S. J. P. Palmer, J. E. Field, J. M. Huntley, Deformation, strengths and strains to failure of polymer bonded explosives, *Proc. Math. Phys. Sci.* **1993**, *440*, 399–419.
[18] P. W. Chen, Y. S. Ding, Mechanical behavior and deformation and failure mechanisms of polymer bonded explosives, *Chin. J. Energet. Mater.* **2000**, *8*, 161–164.
[19] R. Berenbaum, I. Brodie, Measurement of the tensile strength of brittle materials, *Br. J. Appl. Phys.* **1959**, *10*, 282–286.
[20] Y. G. Zhao, H. Fu, Y. L. Li, R. Chen, S. G. Wen, Dynamic tensile mechanical properties of three types of PBX, *Chin. J. Energet. Mater.* **2011**, *19*, 194–199.
[21] MIL-STD-1751, Military standard: safety and performance tests for qualification of explosives, **1982**.
[22] J. Y. Zhang, X. Y. Guo, J. J. Jiao, P. Zhang, Phase transitions of ε-HNIW in compound systems, *AIP Adv.* **2016**, *6*, 11793.
[23] R. Turcotte, M. Vachon, Q. S. M. Kwok, R. Wang, D. E. G. Jones, Thermal study of HNIW (CL-20), *Thermochim. Acta* **2005**, *433*, 105–11

Manuscript received: August 26, 2018
Revised manuscript received: November 20, 2018
Version of record online: January 11, 2019

 © 2019 Wiley-VCH Verlag GmbH & Co. KGaA, Weinheim